



Open Archive TOULOUSE Archive Ouverte (OATAO)

OATAO is an open access repository that collects the work of Toulouse researchers and makes it freely available over the web where possible.

This is an author-deposited version published in : <http://oatao.univ-toulouse.fr/>
Eprints ID : 15549

To link to this article : DOI:10.1021/acs.langmuir.5b04218
URL : <http://dx.doi.org/10.1021/acs.langmuir.5b04218>

<p>To cite this version : Sendekie, Zenamarkos Bantie and Bacchin, Patrice <i>Colloidal Jamming Dynamics in Microchannel Bottlenecks</i>. (2016) Langmuir, vol. 32 (n° 6). pp. 1478-1488. ISSN 0743-7463</p>

Any correspondence concerning this service should be sent to the repository administrator: staff-oatao@listes-diff.inp-toulouse.fr

Supplementary Information

Colloidal Jamming Dynamics in Microchannel Bottlenecks

*Zenamarkos B. Sendekie^{a, b, *} and Patrice Bacchin^{a, b}*

^aUniversité Toulouse III, Laboratoire de Génie Chimique, 118 Route de Narbonne, F-31062
Toulouse, France

^bCNRS, UMR 5503, F-31062, Toulouse, France

*To whom correspondence should be addressed: sendekie@chimie.ups-tlse.fr

1 Microseparator Fabrication and Characteristics

Microfluidic devices mimicking filters with a network of 10 micrometers channels are fabricated with OSTEmerX 322 crystal by soft lithography and replica molding techniques (Whitesides¹). Such devices allow to realize separation of microparticles with real time visualization at pore scale through an optical microscope.

The fabrication process begins by designing the patterns of the microchannels using CleWin 4 software. Photolithography process is used to produce chrome mask with prints of the design. The chrome mask is used as a photomask in contact photolithography to produce a negative relief of SU-8 photoresist on silicon wafer, which is used for casting the microchannels with PDMS. The two components of PDMS (the base and the curing agent) are thoroughly mixed to make sure that the curing agent is uniformly distributed before pouring onto the SU-8 mold. The mixture, filled with air bubbles created during the mixing, is degassed for an hour using a

desiccator to make the trapped air bubbles escape before curing. The PDMS is then poured onto the SU-8 mould and degassed again for half an hour to remove the bubbles created during the pouring and cured at 80°C for an hour. After cooling down to atmospheric temperature, the PDMS mould is carefully peeled-off from the SU-8 mould and is used for replicating the patterns with OSTEmerX 322 crystal on a glass slide.

For replicating the patterns, a thin layer of the crystal polymer is first formed on the glass slide and the PDMS mould is placed atop of it and exposed to UV for 7 seconds. The PDMS mould is then carefully peeled-off and this replicates the microchannel patterns from the PDMS mould to the crystal layer on the glass slide and gives the three sides of the microchannels. To complete the process, a glass cover, with drilled inlet and outlet, is aligned and pressed manually to bond it with the crystal layer. The complete OSTEmerX 322 chip with glass cover is exposed to heat at 100°C for an hour to strengthen the bonding between the glass cover and the crystal layer. This microfluidic device consists of a main channel (1.7 mm wide) followed by an array of parallel, narrow channels at the middle with widths of 10 µm. The height of the microchannels and the main channel is 50 µm. The converging and diverging sections of the main channel are designed to homogenize the suspension before flowing through the microchannels. The filtering part of the device consisted in parallel arrangement of 29 microchannels. Microports (connectors) are glued on the inlet and outlet of the main channel to which tubes (1581 PEEK tubing, 1/32" OD, 0.010" ID, Fluigent) are connected and this gives the complete microfluidic device used for the filtration experiment (Figure S1). This system allows us to have side view of the pore clogging and the cake formation phenomena by using digital video microscopy and hence to investigate a large number of clogging events simultaneously.

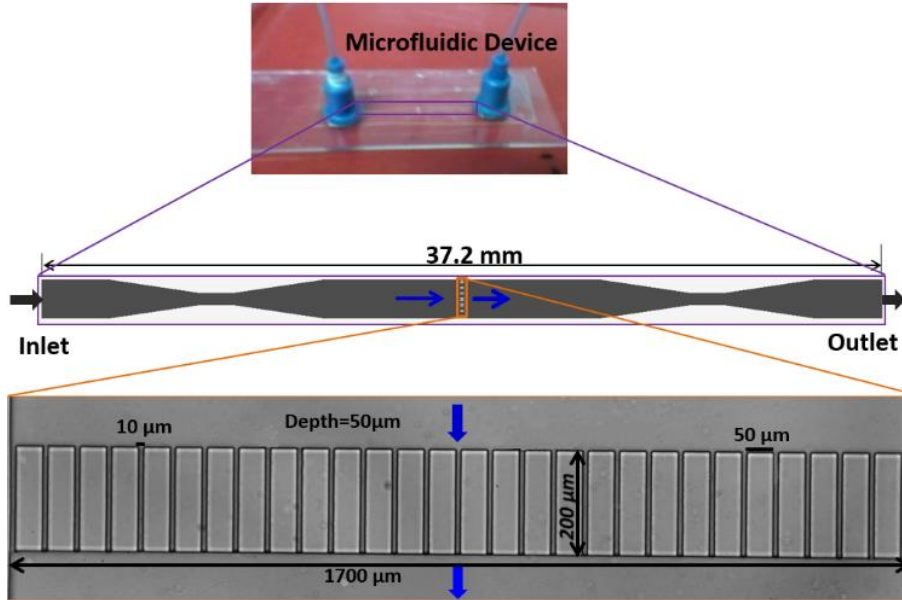


Figure S1. Microfluidic device used for filtration experiment. The inset images show one of the device designs with square corners at the channel entrance in full view of parallel array of microchannels. The microchannels have $10\ \mu\text{m}$ width and a uniform depth of $50\ \mu\text{m}$. The width of the rectangular pillars is $50\ \mu\text{m}$. The entire length of the channel is $37.2\ \text{mm}$ and the width of the main channel is $1.7\ \text{mm}$.

2 Filtration Experiments

Filtration experiments are performed in dead-end mode at both constant pressure and constant flow rate by using Microfluidic Flow Control System (MFCS) and Flowell (from Fluigent). The suspension is continuously injected into the device at controlled flow rate or pressure. The MFCS is connected to external pressure source (compressed air) and regulates the pressure supply to the reservoirs. The suspension is pushed from the reservoirs pneumatically to the flow sensors on the Flowell and then to the microfluidic device which is placed on the platform of an Axiolab (Zeiss) microscope. The filtration process is recorded by using highly light sensitive camera (Pixelfly QE, PCQ) which is connected to a computer for image storage, data processing

and results analysis. The exposure time for the camera was 6 milliseconds. The dynamics of the particle capture and deposit formation are recorded by taking images every 10 seconds during filtration. Filtration data (flowrate, pressure and permeate volume) are recorded every 10 seconds by using MAESFLO software (Fluigent). The experimental setup for capturing images and recording the pore clogging phenomena is shown in Figure S2.

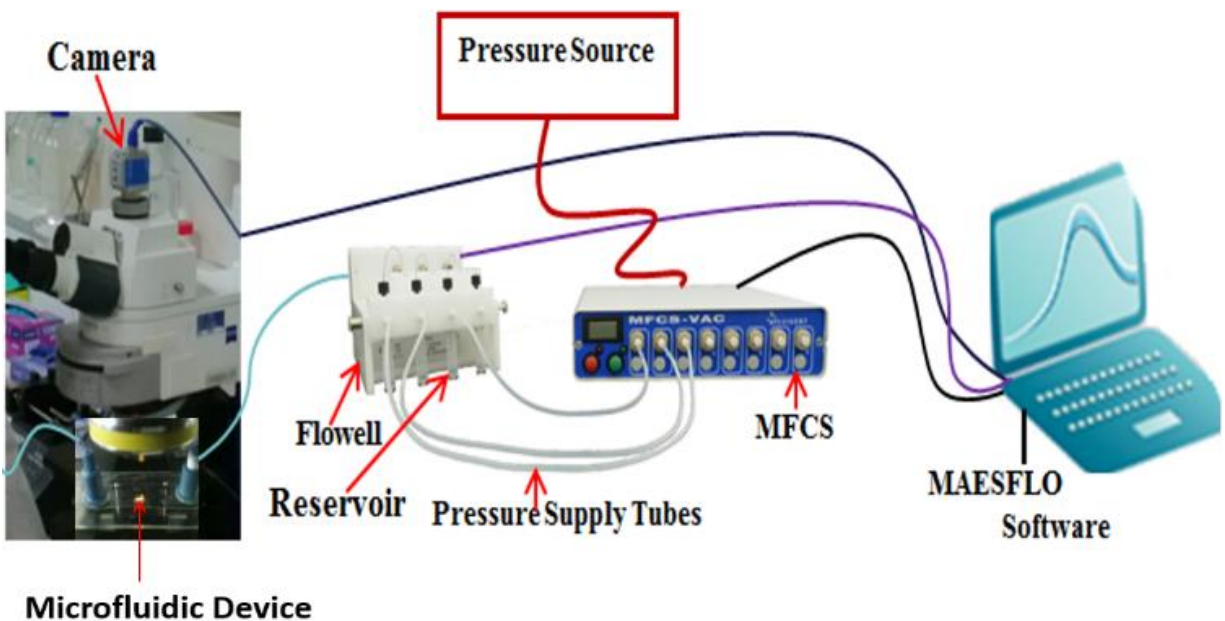


Figure S2. Experimental setup for recording and imaging the pore clogging and deposit formation phenomena. The suspension in the reservoir is pushed through the flow sensors in the Flowcell to the microfluidic filter by the pressure applied by the MFCS through the pressure supply tubes. Images are captured by the camera for studying the local capture dynamics and the pressure and the flow rate are recorded by the MAESFLO software for studying the filtration permeability dynamics.

3 Determination of Fouling Rate

The determination of the slope for each constant flow rate run (i.e., for 5, 10, 15 ...70 $\mu\text{L}/\text{min}$) in the flow stepping experiments is demonstrated in figure S3. This slope determination enables us to evaluate the fouling rate.

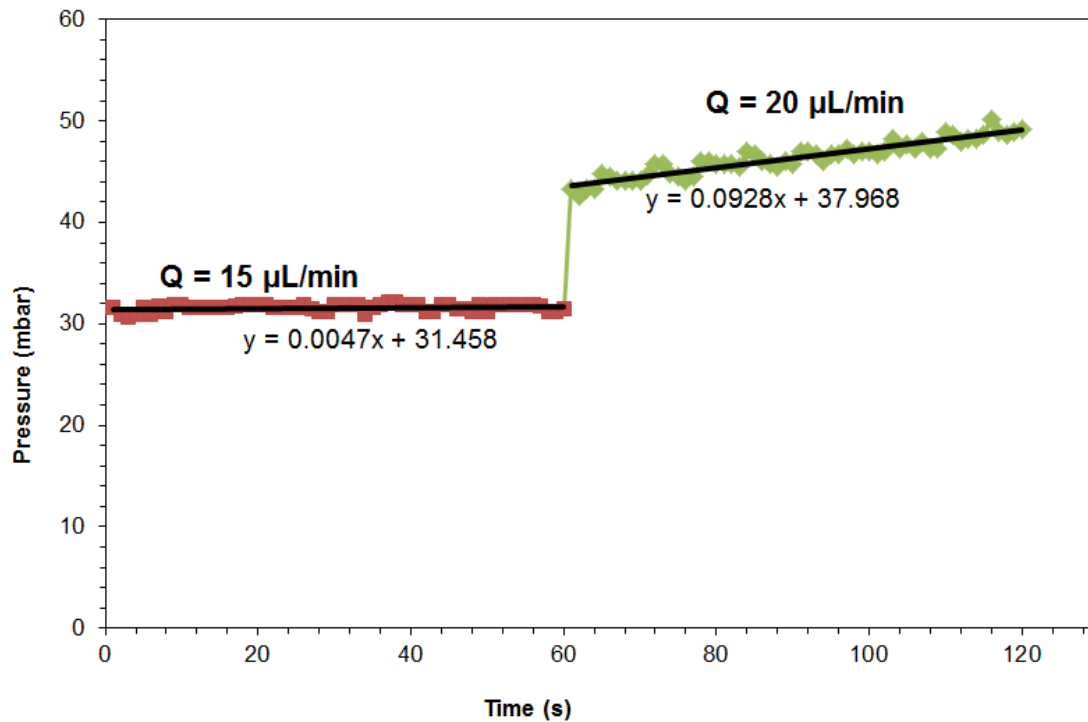


Figure S3. Demonstration of how the slopes are calculated for each constant flow rate run in the flow stepping experiments to evaluate the fouling rate. This demonstration is for the 0.01 mM ionic strength suspension for flow rates of 15 $\mu\text{L}/\text{min}$ and 20 $\mu\text{L}/\text{min}$.

4 DLVO Interactions Calculations

From the classical DLVO theory, the colloidal interaction energy can be calculated as the sum of the van der Waals attraction energy (U_A) and the electrostatic repulsive interaction (U_R) as follows:

$$U = U_A + U_R \quad (1)$$

To compute the van der Waals attraction, the modified Hamaker relation is used:¹

$$U_A = -\frac{A_H}{6} \left\{ \frac{2}{l^2-4} + \frac{2}{l^2} + \ln \left[1 - \frac{4}{l^2} \right] \right\} \quad (2)$$

where A_H is the Hamaker constant with a value of 1.3×10^{-20} J for polystyrene particles² and $l=r/R_p$ with r the interparticle centre-to-centre distance and R_p the particle radius.

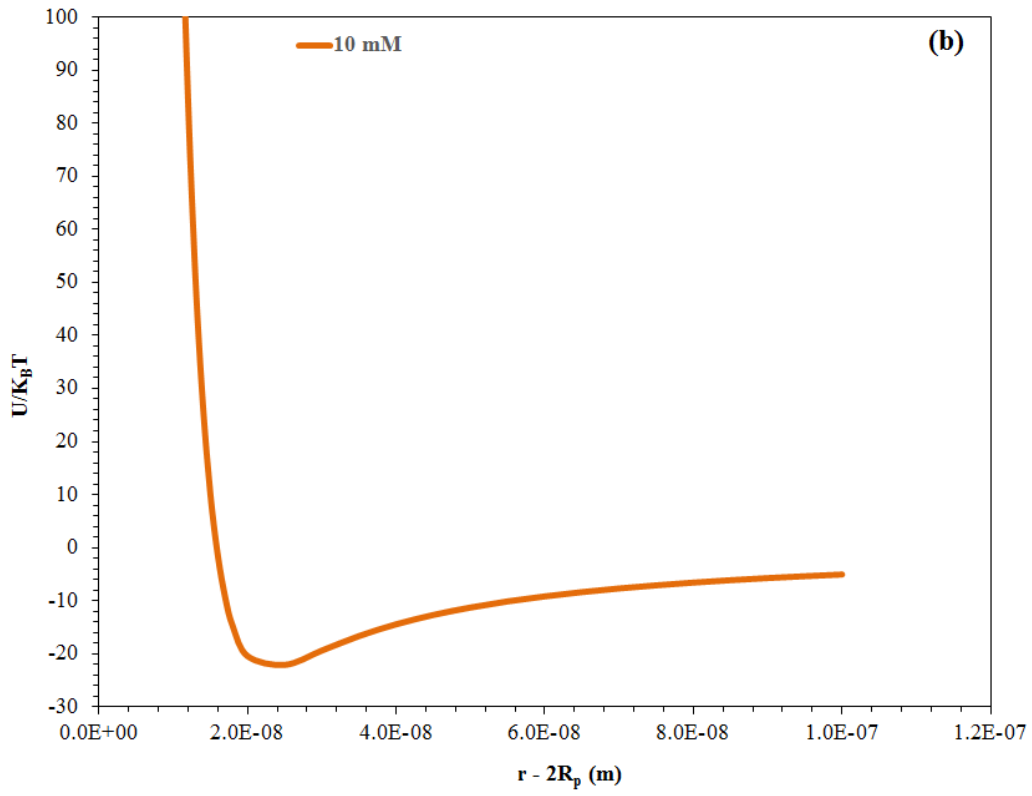
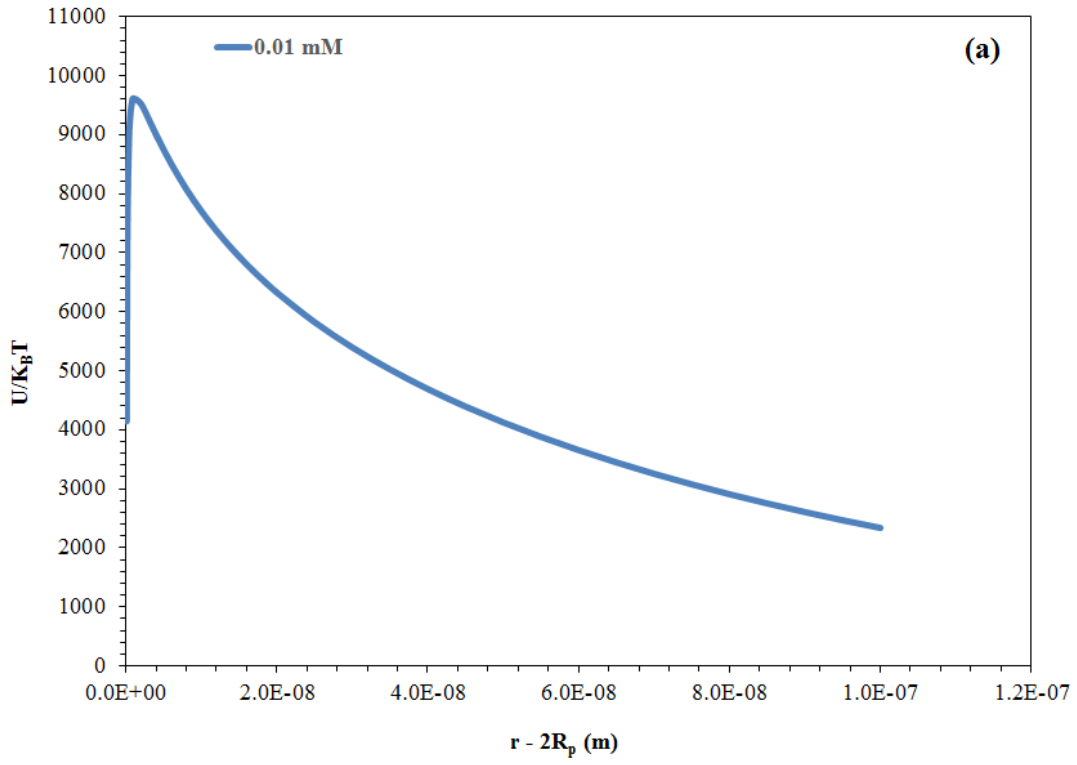
To compute the electrostatic repulsive interaction, the modified Hogg-Healy-Fuersteneau expression derived by Sader et al. (1995) for high surface potential is used.³

$$U_R = 4\pi\epsilon \left(\frac{K_B T}{e_1} \right)^2 \left\{ 4 e^{\frac{\kappa(r-2R_p)}{2}} \tanh^{-1} \left[e^{-\frac{\kappa(r-2R_p)}{2}} \tanh \left(\frac{\psi_o e_1}{K_B T} \right) \right] \right\}^2 \frac{R_p^2}{r} \ln[1 + e^{-\kappa(r-2R_p)}] \quad (3)$$

where ϵ ($=6.95 \times 10^{-10}$ CV⁻¹m⁻¹) the permittivity of the medium, ψ_o ($=-57$ mV) the surface potential, and k the reciprocal Debye length, defined as:

$$\kappa = (N_A e^2 \sum_i C_i z_i^2 / \epsilon_r \epsilon_o K_B T)^{1/2} \quad (4)$$

where N_A ($=6.022 \times 10^{23}$ mol⁻¹) is the Avogadro constant, C_i the bulk concentration of the i^{th} ion, z_i the charge valence of the i^{th} ion, e (1.602×10^{-19} C) the electron charge, ϵ_r ($=78.54$ for water at room temperature) is the relative dielectric constant of the dispersion medium, ϵ ($=8.854 \times 10^{-12}$ CV⁻¹m⁻¹) the permittivity of vacuum, K_B ($=1.38 \times 10^{-23}$ m²Kgs⁻²K⁻¹) the Boltzmann constant, and T the absolute temperature. Using these sets of equations, we are able to calculate the secondary energy minima and the potential barrier maxima for each ionic strength suspensions, which are presented in the paper in table 1.



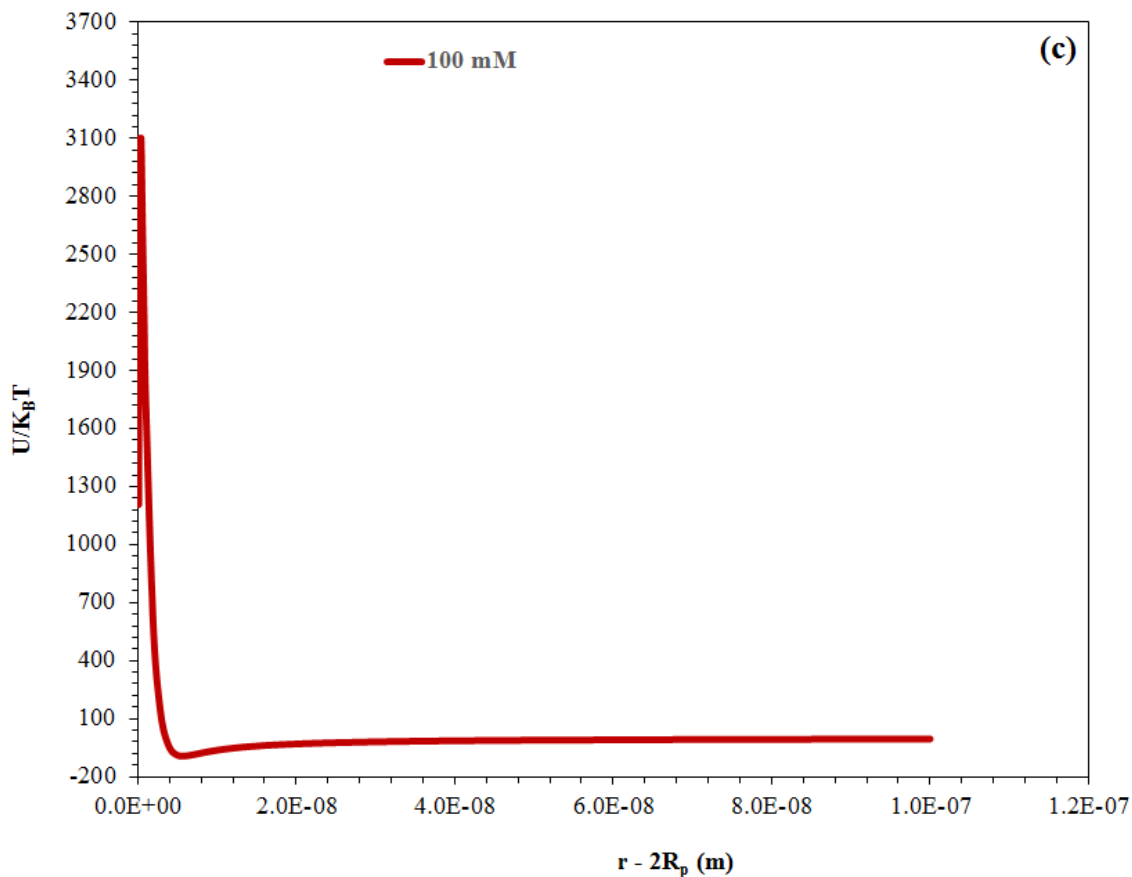


Figure S4. Interaction potential energy curves plotted as a function of the surface-to-surface distance between the particles ($h=r-2R_p$) showing the different interaction profiles and their importance for three different ionic strength conditions. (a) 0.01 mM, (b)10 mM, (c)100 mM.

References

- (1) Vanni, M.; Baldi, G. Coagulation efficiency of colloidal particles in shear flow. *Adv. Colloid Interface Sci.* **2002**, 97, 151.
- (2) S. H. Maron, M. E. Elder and I. N. Ulevitch, Determination of surface area and particle size of synthetic latex by adsorption VI. Critical micelle concentrations of various emulsifiers in latex. *J. Colloid Sci.*, **1954**, 9, 89.
- (3) J. E. Sader, S. L. Carnie and D. Y. C. Chan, Accurate Analytical Formulas for the Double Layer Interaction between Spheres. *J. Colloid Interface Sci.*, **1995**, 171, 46.